TNP-470, an angiogenesis inhibitor, suppresses the progression of peritoneal fibrosis in mouse experimental model

Yoko Yoshio, Masanobu Miyazaki, Katsushige Abe, Tomoya Nishino, Akira Furusu, Yohei Mizuta, Takashi Harada, Yoshiyuki Ozono, Takehiko Koji, and Shigeru Kohno

Second Department of Internal Medicine, Division of Renal Care Unit; Department of General Medicine; and Department of Histology and Cell Biology, Nagasaki University School of Medicine, Nagasaki, Japan

TNP-470, an angiogenesis inhibitor, suppresses the progression of peritoneal fibrosis in mouse experimental model.

Background. In patients on long-term peritoneal dialysis (PD), angiogenesis and vasculopathy are observed in the peritoneum, and the degree of vascularization correlates with the area of fibrotic tissue, suggesting the involvement of angiogenesis in the progression of peritoneal fibrosis. The aim of the present study was to evaluate the effect of TNP-470, an anti-angiogenic compound, on the development of peritoneal fibrosis induced by chlorhexidine gluconate (CG).

Methods. Peritoneal fibrosis was induced by injection of CG into peritoneal cavity of Institute for Cancer Research (ICR) mice. TNP-470 was injected subcutaneously with CG. Mice were sacrificed, and peritoneal tissues were dissected out at days eight and 16 after CG and TNP-470 injection. The expression patterns of CD31 (as a marker of endothelial cells), vascular endothelial cell growth factor (VEGF), α-smooth muscle actin (as a marker of myofibroblasts), heat shock protein 47 (HSP47), type III collagen, F4/80 (as a marker of mice macrophages), proliferating cell nuclear antigen (PCNA), and cyclin-dependent kinase 2 (Cdk2) were examined by immunohistochemistry.

Results. CG-injected mice showed thickening of the submesothelial zone and increased number of vessels, myofibroblasts, and infiltrating macrophages. The expression levels of VEGF, type III collagen, and HSP47 were increased, and a large number of PCNA-positive cells and Cdk2-expressing cells were observed in the thickened submesothelial area. Treatment with TNP-470 suppressed the submesothelial zone thickening and reduced collagen III expression as well as angiogenesis. TNP-470 also decreased the number of VEGF-expressing cells, myofibroblasts, macrophages, PCNA-positive cells, and Cdk2-expressing cells.

Conclusion. Our results indicate the involvement of angiogenesis in the progression of peritoneal fibrosis, and suggest that TNP-470 may be potentially useful for the prevention of peritoneal fibrosis through inhibition of angiogenesis and suppression of myofibroblast proliferation.

Peritoneal dialysis (PD) is a beneficial therapy for end-stage renal disease (ESRD), but long-term use of PD induces histopathologic changes in the peritoneum, such as peritoneal fibrosis with increased submesothelial collagen deposition and loss of mesothelial cells [1–5]. Recent studies also demonstrated increased peritoneal vascularization with vasculopathy in patients on long-term PD [3, 6–8]. Furthermore, Honda et al [6] reported the development of submesothelial fibrosis and indicated that at that stage, the appearance of vasculopathy correlated with a reduction in ultrafiltration. Williams et al [5] also demonstrated that the prevalence of vasculopathy increased with long-term use of PD, and that the number of blood vessels in the peritoneum correlated with the amount of fibrous tissue in PD patients on peritoneal fibrosis. Other studies showed that the concentration of vascular endothelial growth factor (VEGF) in the peritoneal fluid was up-regulated in PD patients [9, 10]. These findings suggest that in peritoneum of PD patients, where the number of blood vessels is increased, angiogenesis is associated with the pathogenesis of peritoneal fibrosis.

Angiogenesis, or formation of new blood vessels, occurs during the progression of various pathologic conditions, such as solid tumor growth [11, 12], diabetic retinopathy [13], and chronic inflammation [14, 15]. It is widely accepted that the inhibition of angiogenesis is a suitable strategy to prevent the progression of those diseases. TNP-470, a synthetic analog of fumagillin, a natural product of *Aspergillus fumigatus*, is known as a potent anti-angiogenic compound [16]. The efficacy of TNP-470 as an angiogenesis inhibitor has been demonstrated experimentally in the treatment of hemangiomas [17], corneal neovascularization [18], collagen-induced arthritis [19, 20], primary tumors, and metastatic diseases [21–24]. While TNP-470 is known to exert its anti-angiogenic effect through the preferential inhibition of endothelial cell proliferation [16, 25], it has been recently demonstrated that this agent also inhibits proliferation of fibroblasts [16, 26], vascular smooth muscle cells [27], hepatic stellate cells [28], and mesangial cells [29].

The present study was designed to determine the effect of TNP-470 on the progression of peritoneal fibrosis using an experimental model of peritoneal fibrosis induced by chlorhexidine gluconate (CG) injection. Although the mechanism underlying the development of peritoneal fibrosis by CG is not clear, previous research showed that persistent chemical irritation by CG could induce tissue damage with inflammation subsequently followed by tissue repair with excessive proliferation of fibroblasts [30]. In addition, we demonstrated previously that during progressing CG-induced peritoneal fibrosis, the number of blood vessels also increased. In the present study, we demonstrated that treatment with TNP-470 reduced the number of blood vessels, VEGF-expressing cells, proliferating cell nuclear antigen (PCNA)-positive endothelial cells and myofibroblasts, and cyclin-dependent kinase 2 (Cdk2)-expressing cells, and suppressed the progression of peritoneal thickening and collagen deposition. Our results indicate that TNP-470 is effective in preventing the progression of peritoneal fibrosis in our model.

METHODS

Animal models

The experiments described in this study were conducted in female ICR mice (Japan SLC Inc., Shizuoka, Japan) of 25 ± 3 g body weight. They were housed in a light- and temperature-controlled room in Biomedical Research Center, Center for Frontier Life Sciences, Nagasaki University. They had free access to laboratory chow and tap water in standard rodent cages. The experimental protocol was inspected by Animal Care and Use Committee of Nagasaki University School, and approved by the President of Nagasaki University School. Peritoneal fibrosis was induced by intraperitoneal injection of 0.1% chlorhexidine gluconate (CG) in 15% ethanol dissolved in saline, as described previously with some modifications [30, 31]. Mice received injections of CG into the peritoneal cavity at a volume of 10 mL/kg body weight every other day (CG group). In another group of mice, TNP-470 (a kind gift from Takeda Chemical Industries, Osaka, Japan) dissolved in saline containing 1% ethanol and 5% gum Arabic (016–00025; Wako Pure Chemical Industries, Osaka, Japan) was injected subcutaneously twice per week at a concentration of 20 mg/kg with CG (CG+TNP470 group). Mice of another group were injected 15% ethanol in saline intraperitoneally (control group). Each group consisted of 10 mice. The effect of repeated injections of TNP-470 alone and the vehicle used to dissolve TNP-470 (saline containing 1% ethanol and 5% gum Arabic) on the progression of peritoneal fibrosis were examined. The dose and interval for TNP-470 injections were selected based on pilot studies conducted to determine the effects of different doses on the thickness of submesothelial area. TNP-470 doses lower than 10 mg/kg/week did not reduce peritoneal thickness compared with nontreated CG mice. Consequently, we selected 20 mg/kg × 2/week for the present study. CG (0.1%) and TNP-470 were injected under ether anesthesia to ensure the injection of the correct dose at the correct site, and to avoid induction of pain during intraperitoneal injection. Mice were sacrificed at days eight or 16 after the first CG and TNP-470 injection, and peritoneal tissues were dissected out carefully. To avoid direct damage to the peritoneum caused by repeated injections, injections of CG were made at the lower part of the peritoneum, while the upper portion of the parietal peritoneum was used for the following examination. Tissues were fixed with 4% paraformaldehyde immediately after sampling and embedded in paraffin.

Histologic and immunohistochemical examination

For morphologic examination, 4-μm thick paraffin-embedded tissues were stained with hematoxylin and eosin (H&E). The following antibodies were used for immunohistochemistry: (*1*) rat antimouse CD31/PECAM-1 antibody diluted 1/50 (1625–01; Southern Biotechnology, Birmingham, AL, USA), which was used as a marker of endothelial cells; (*2*) horseradish peroxidase (HRP)–labeled-dextran polymer-conjugated mouse anti-α-smooth muscle actin (SMA) antibody (U7033; Dako, Glostrup, Denmark), which was used as a marker of myofibroblasts; (*3*) rabbit anti-type III collagen antibody diluted 1/200 (LB-1393; LSL Co., Tokyo, Japan); (*4*) mouse anti-heat shock protein (HSP) 47 antibody diluted 1/50 (StressGen, Victoria, British Columbia, Canada), which is a molecular chaperone necessary for production of collagen; (*5*) HRP-labeled dextran polymer-conjugated mouse anti-PCNA antibody (U7032; Dako) as a marker of proliferating cells; (*6*) rabbit anti-VEGF antibody diluted 1/100 (sc-507; Santa Cruz Biotechnology, Santa Cruz, CA, USA); (*7*) rat anti-F4/80 antibody diluted 1/100 (MCA497; Serotec, Oxford, UK) as a marker of mouse macrophages; and (*8*) mouse anti-Cdk2 antibody, a marker of cell cycle progression, diluted 1/50 (610145; BD Transduction Laboratories, San Diego, CA, USA).

Indirect immunohistochemical technique was used for type III collagen, HSP47, F4/80, and Cdk2. Deparaffinized tissue sections were incubated for 30 minutes with a blocking buffer containing 5% normal goat serum, 5% fetal calf serum, 5% bovine serum albumin, and 20% normal swine serum in phosphate-buffered saline (PBS). The sections were then reacted with the primary antibody, and diluted in the same blocking buffer. After reacting with anti-type III collagen antibody for one hour at room temperature, sections were reacted with HRP-conjugated swine antirabbit immunoglobulin antibody (P0399; Dako) diluted 1/50 for 30 minutes at room

temperature, and a complex of rabbit anti-HRP antibody and HRP (Z0113; Dako) diluted 1/100 for 30 minutes at room temperature. For HSP47 and Cdk2, sections were reacted with a complex of anti-HSP47 antibody and HRP-conjugated rabbit antimouse immunoglobulin antibody (Z0109; Dako) diluted 1/100, or a complex of anti-Cdk2 antibody and HRP-conjugated rabbit antimouse immunoglobulin antibody diluted 1/100 for one hour at room temperature, and HRP labeled-dextran polymer-conjugated goat antirabbit immunoglobulin antibody (K4002; Dako) for 30 minutes at room temperature. For F4/80, sections were reacted with HRP-conjugated rabbit antirat immunoglobulin antibody (Z0147; Dako) and HRP-conjugated swine antirabbit immunoglobulin antibody after reacting with anti-F4/80 antibody for one hour at room temperature. We used direct immunohistochemical technique for α-SMA and PCNA staining. After deparaffinization, the sections were incubated for 30 minutes with a blocking buffer similar to that described above, and then reacted with anti-α-SMA antibody or anti-PCNA antibody for 1 hour at room temperature. For CD31 and VEGF staining, deparaffinized tissues were stained with avidin-biotin complex technique using Vectastain Elite ABC kit (Vector Laboratories, Burlingame, CA, USA) after reacting with first antibody for 16 hours at 4°C. Reaction products were visualized by treating sections with H_2O_2 and 3–3 diaminobenzidine tetrahydrochloride. Finally, the sections were counterstained with methyl green and mounted. For all specimens, negative controls were prepared with irrelevant mouse monoclonal antibody, rat monoclonal antibody, or the normal rabbit IgG in place of the primary antibody.

Double staining for CD31 and PCNA was also performed. After the CD31 staining step as described above, sections were washed in PBS to stop the color reaction, and incubated with double staining enhancer (50–056; Zymed Laboratories, Inc., San Francisco, CA, USA). Thereafter, they were reacted with anti-PCNA antibody followed by incubation with HRP-conjugated antibodies as mentioned above. A second chromogen, True blue (71–00-64; KPL, Gaithersburg, MD, USA) was then applied, which stained positive cells in blue. The tissue sections were not counterstained with methyl green because this counterstaining could interfere with the color from the chromogen.

Morphometric analysis

To assess the extent of peritoneal thickening, we used digitized images and image analysis software (Win ROOF MITANICORP, Chiba, Japan). We measured the thickness of the submesothelial zone above the abdominal muscle in cross-sections of the abdominal wall. The image was transformed into a matrix of 1280 × 1000 pixels and viewed at ×100 magnification. We selected a width of 840 μm in the examined field under the microscope and measured the area of the submesothelial layer within the selected width of 840 μm. For each sample, eight such areas were selected and the average area of the submesothelial layer was determined.

In each peritoneal sample, the numbers of CD31-positive vessels, α-SMA–expressing cells, HSP47-expressing cells, PCNA-positive cells, VEGF-expressing cells, F4/80-positive macrophages, and Cdk2-expressing cells were counted in 10 fields at ×400 magnification. We also counted the number of cells double-positive for CD31 and PCNA at 10 fields under ×400 magnification in each group, and calculated the percentage of double-positive cells in CD31-expressing cells.

Statistical analysis

Data are expressed as mean ± SD. Differences among groups were examined for statistical significance using repeated measures analysis of variance (ANOVA) (Bonferroni/Dunn test). A *P* value less than 0.05 denoted the presence of statistically significant difference.

RESULTS

Morphologic examination

Morphologic changes were assessed by H&E staining. In the normal mouse, the peritoneal tissue consisted of peritoneal mesothelial monolayer and exiguity of connective tissues under the mesothelial layer (Fig. 1A). The peritoneal samples of mice of the CG group showed marked thickening of the submesothelial compact zone and the presence of numerous cells. The submesothelial zone showed progressive thickening to day 16 (day eight; Fig. 1B, day 16; Fig. 1C). At day eight, there were no appreciable differences in the submesothelial zone thickness between the CG and CG+TNP-470 groups (Figs. 1D and 2). At day 16, the thickness of the submesothelial zone and the number of infiltrating cells in CG+TNP-470-treated mice were significantly less than those of CG-treated mice (Figs. 1E and 2). Peritoneal tissues of control mice were almost normal without any thickening of the submesothelial zone (Fig. 1F). Repeated injections of TNP-470 alone did not affect the thickening of the peritoneum compared with the control (Fig. 1G) and the severity of submesothelial area thickening in mice injected with CG and the vehicle used to dissolve TNP-470 was similar to that in CG injected mice (Fig. 1H).

Expression of CD31 and VEGF

Recent studies described the presence of increased number of vessels in thickened peritoneal tissues of peritoneal dialysis (PD) patients [5, 8] and animal models
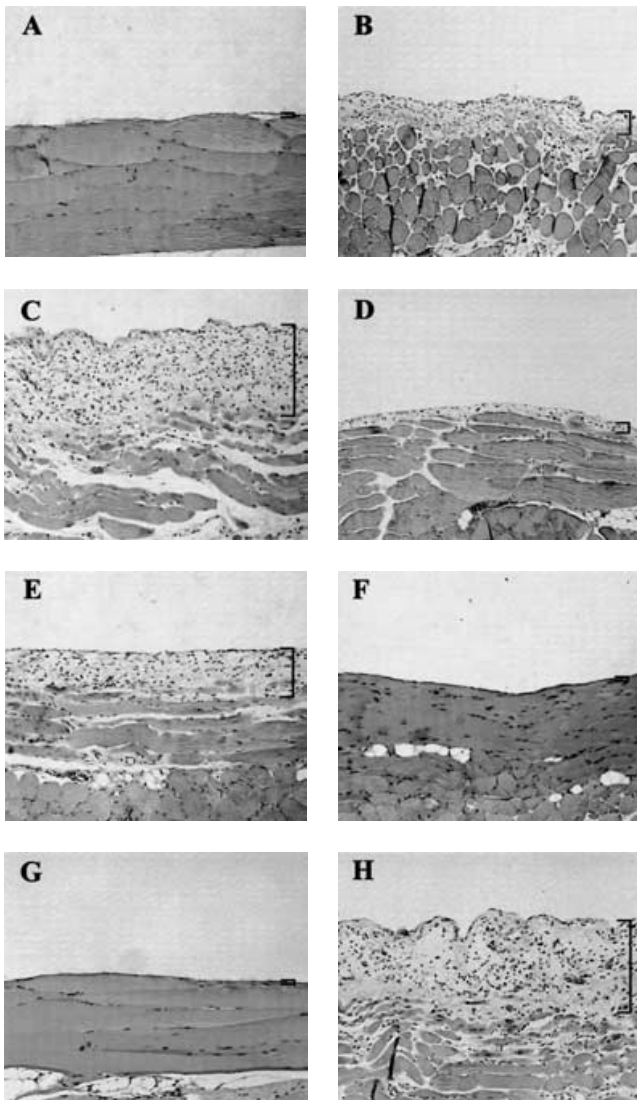
Fig. 2. The area of submesothelial fibrotic tissue in control group, CG group, and CG+TNP470-treated group at day 8 (left) and day 16 (right). Data are mean ± SD. The area of submesothelial fibrotic tissue was measured with the range of 840 μm. Submesothelial area in CG group is significantly increased compared with control group at days 8 and 16, while administration of TNP-470 significantly reduced the progression of submesothelial thickening in CG+TNP470 group at day 16. *$P <$ 0.01 vs. control. **$P <$ 0.05 vs. control. #$P <$ 0.01 vs. CG-treated mice.

Fig. 1. Hematoxylin and eosin staining of peritoneal tissues. In normal mice, note the monolayer of mesothelial cells covered with the surface of peritoneum (*A*). Chlorhexidine gluconate (CG) injection induced significant thickening of the peritoneum at days 8 (*B*) and 16 (*C*). Administration of TNP-470 in CG-treated mice significantly suppressed the progression of peritoneal thickening at day 16 (*E*) but not at day 8 (*D*). In control mice injected with 15% ethanol/saline, the peritoneum is only slightly thickened at day 16 (*F*). Repeated injections of TNP-470 without CG had no effect on peritoneal thickening compared with control mice (*G*), and injection of the vehicle used for dissolving TNP-470 with CG did not alter the thickening of peritoneum compared to mice injected with CG alone (*H*). Bars, the area of submesothelial compact zone. Magnification: ×100.

Fig. 3. Immunohistochemistry for CD31 and VEGF at day 16. Note the presence of numerous vessels positively stained for CD31 (arrowheads) in CG group (*A*), while a few vessels are stained for CD31 (arrowheads) in CG+TNP470 group (*B*). Magnification: ×300. Note the large number of VEGF-expressing cells in the CG group (*C*). VEGF-positive cells were peritoneal mesothelial cells (*E*), vascular endothelial cells (*F*), and fibroblast-like cells (*G*). TNP-470 treatment markedly decreased the number of these cells (*D*) in the thickened submesothelial zone. Magnification: (C and D): ×200; (E, F, and G): ×800.

of experimental peritoneal fibrosis [30, 32]. Therefore, we quantified the number of blood vessels using immunohistochemistry for CD31. The number of CD31-positive vessels was markedly increased in mice of the CG group (Fig. 3A). TNP-470 administration decreased the number of CD31-expressing vessels (Fig. 3B). We also examined VEGF expression in the submesothelial area. In the control group, VEGF was expressed in
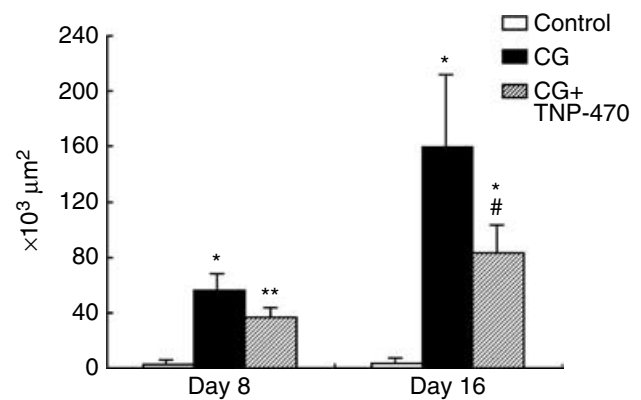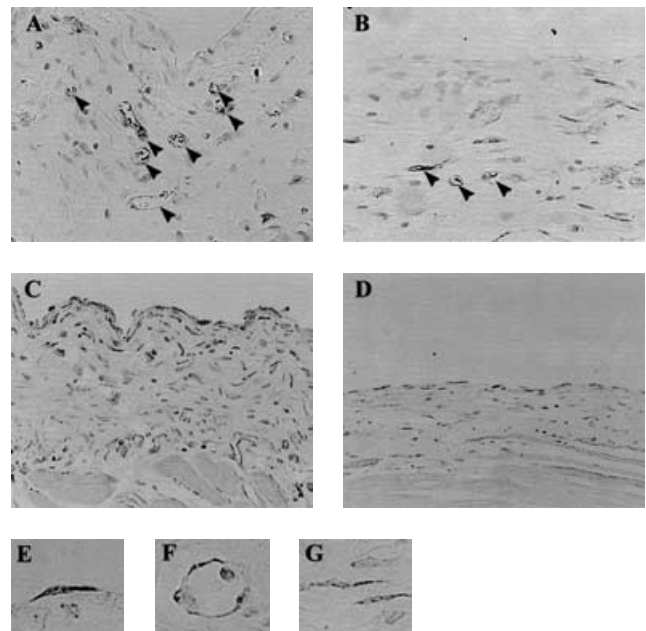
the peritoneal mesothelial monolayer (data not shown). Treatment with CG markedly increased the number of VEGF-expressing cells compared with the control, and the types of cells positive for VEGF were peritoneal mesothelial cells (Fig. 3E), vascular endothelial cells (Fig. 3F), and spindle-shaped fibroblasts (Fig. 3G).

Table 1. Results of immunohistochemistry for CD31, VEGF, α-SMA, HSP47, and F4/80

	Number of positive cells in the peritoneum		
	Control group	CG group	CG+TNP470 group
CD31	0.6 ± 0.6	32.4 ± 7.4^a	16.6 ± 6.4^b
VEGF	20.6 ± 5.2	205.8 ± 52.4^a	82.3 ± 18.9^b
α-SMA	6.3 ± 2.7	203.4 ± 69.0^a	79.6 ± 38.0^b
HSP47	23.7 ± 4.4	207 ± 20.9^a	82.8 ± 18.2^b
F4/80	0.7 ± 1.0	45.4 ± 9.8^a	16.8 ± 6.0^b

Data are mean ± SD. The numbers of CD31-positive vessels, VEGF-expressing cells, α-SMA–expressing cells, HSP47-expressing cells, and F4/80-positive cells were determined in 10 fields of the submesothelial region selected at random in each mouse and examined at ×400 magnification.

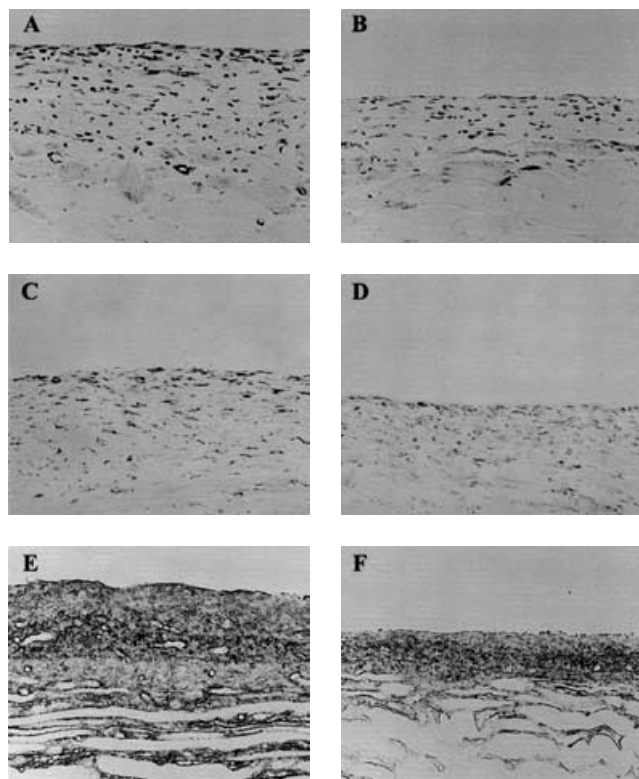[a] $P < 0.01$ vs. control group.
[b] $P < 0.01$ vs. CG group.

Fig. 5. Immunohistochemistry for F4/80 at day 16. F4/80-expressing cells are present in thickened peritoneal tissues in CG group (*A*). Compared with CG group, the number of F4/80-positive cells is reduced in CG+TNP470 group (*B*). Magnification: ×200.

Fig. 4. Immunohistochemistry for α-SMA (*A* and *B*), HSP47 (*C* and *D*), and type III collagen at day 16 (*E* and *F*). In CG group, note the presence of a large number of α-SMA–positive cells in the submesothelial zone at day 16 (A). The number of α-SMA is reduced in CG+TNP470 group (B). Note the strong expression of HSP47 in the thickened submesothelial in CG group (C), while such expression is decreased in CG+TNP470 group at 16 days (D). In CG group, type III collagen is strongly expressed in the submesothelial compact zone (E), but it is clearly decreased in CG+TNP470 group at day 16 (F). Magnification: ×200.

Meanwhile, peritoneal tissues of CG+TNP-470 mice contained fewer VEGF-expressing cells in the submesothelial zone compared with the CG-treated mice (Fig. 3D). Table 1 summarizes the results of quantitative analysis of CD31-positive vessels and VEGF-expressing cells in the submesothelial zone at day 16 for the three groups.
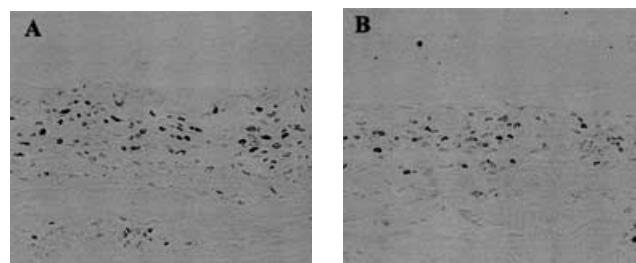
Expression of α-SMA, HSP47, and type III collagen

The results of immunohistochemical analyses for α-SMA, HSP47, and type III collagen at day 16 are shown in Figure 4 and Table 1. In the control group, the expression of α-SMA was only observed in vascular smooth muscle cells (data not shown). In contrast, in mice of the CG group, α-SMA expression was found in myofibroblasts in addition to vascular smooth muscle cells, and numerous α-SMA–expressing myofibroblasts were identified in the thickened peritoneal tissues (Fig. 4A). Compared with the CG group, the number of α-SMA–positive myofibroblasts was markedly reduced in the CG+TNP-470 group (Fig. 4B). Similarly, HSP47 expression was limited to mesothelial cells in the control group (data not shown). In CG group, the number of HSP47-positive cells was higher, and most of HSP47-positive cells were mesothelial cells and spindle-shaped fibroblasts in the thickened submesothelial zone, based on morphologic criteria (Fig. 4C). Treatment of mice with CG and TNP-470 resulted in reduction of HSP47-positive cell count in the peritoneum, compared with the CG group (Fig. 4D, Table 1). We also investigated the peritoneal expression of type III collagen by immunohistochemistry. In the CG group, type III collagen was diffusely expressed in the submesothelial zone (Fig. 4E), while TNP-470 treatment reduced type III collagen expression (Fig. 4F).

Expression of F4/80, PCNA, and Cdk2

To identify the type of cells infiltrating the submesothelial zone, we stained sections with anti-F4/80 antibody, a marker of mouse macrophages. In CG group, a large number of F4/80-positive macrophages was observed in the thickened peritoneal tissues compared with the control (Fig. 5A, Table 1), while TNP-470 treatment markedly reduced their number (Fig. 5B).

We also examined the antiproliferative effect of TNP-470 in peritoneal fibrosis by PCNA staining. Treatment with CG resulted in the appearance of numerous PCNA-positive cells in the thickened submesothelial area
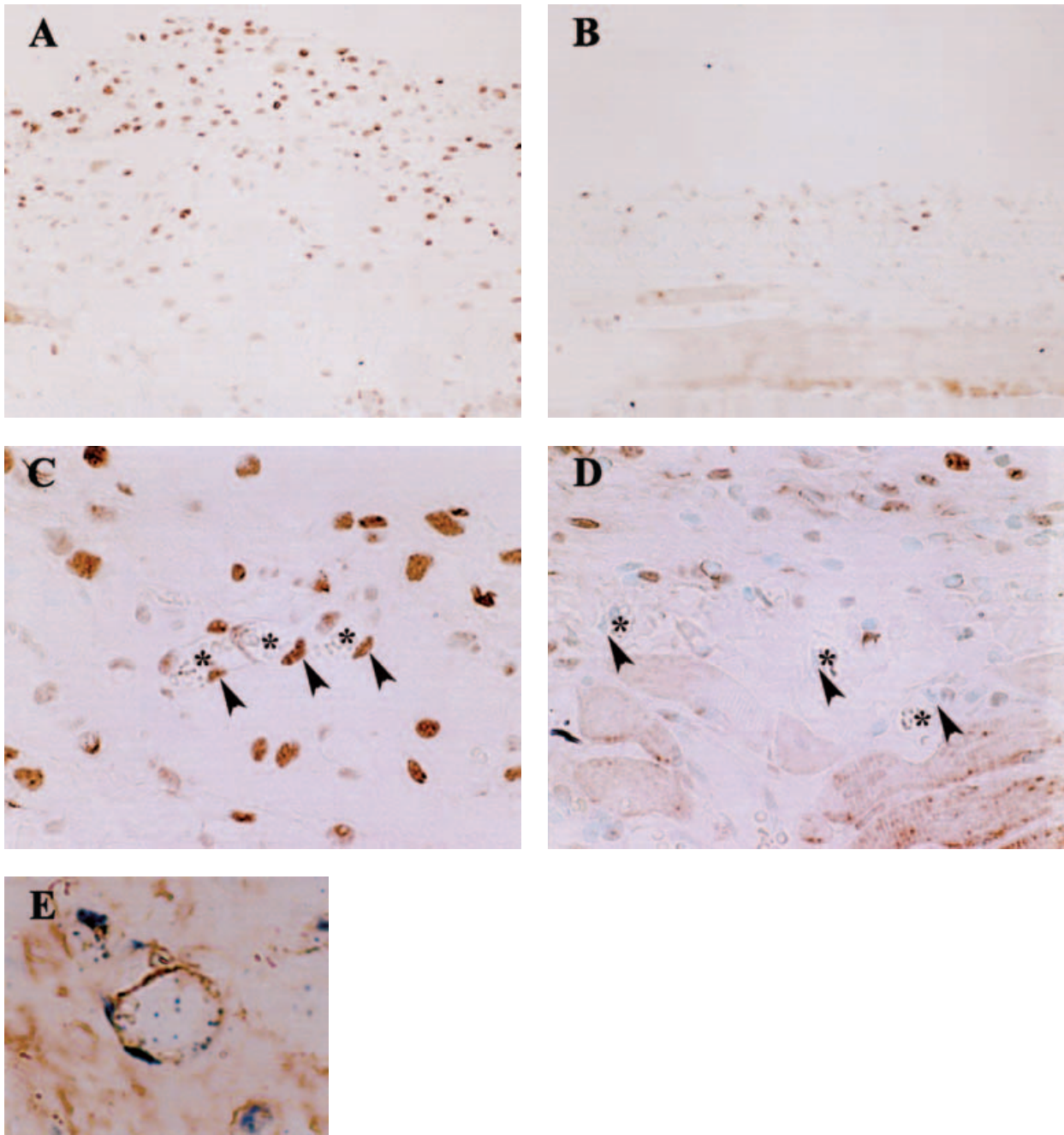
Fig. 6. Immunohistochemistry for PCNA. In CG group, note the strong expression of PCNA positive cells in the markedly thickened submesothelial area (*A*) and among vascular endothelial cells (arrowheads) (*C*). Cells positive for PCNA were decreased in number in the submesothelial area in CG+TNP470 group at 16 days (*B*), especially in vessels (arrowheads) (*D*). Double staining for CD31 (brown) and PCNA (blue) in the same section. Note that CD31-positive cells are also positive for PCNA (*E*). Magnification: (A and B): ×100; (C and D): ×400; (E): ×800. *Vessels.

(Fig. 6A), and those cells were peritoneal mesothelial cells, fibroblast-like spindle-shaped cells, and vascular endothelial cells (Fig. 6C). Compared with CG group, treatment with TNP-470 significantly reduced the number of PCNA-expressing cells (Fig. 6B), especially vascular endothelial cells (Fig. 6D, Table 2), in peritoneal tissues. We also examined the antiproliferative effect of TNP-470 on endothelial cells using double staining for CD31

and PCNA (Fig. 6E). In the CG group, $72.9 \pm 6.6\%$ of CD31-positive cells were stained for PCNA in the submesothelial zone, while only $27.6 \pm 7.5\%$ of CD31-positive cells expressed PCNA in TNP-470 group. With regard to Cdk2 expression, the number of Cdk2-expressing cells in the CG group was higher than the control (Fig. 7A). Cdk2 expression was identified on vascular endothelial cells, spindle-shaped fibroblasts, and some mesothelial

Table 2. Results of immunohistochemistry for PCNA, double staining for PCNA/CD31, and immunohistochemistry for Cdk2

	Number of positive cells in the peritoneum		
	Control group	CG group	CG+TNP470 group
PCNA	9.3 ± 3.8	244.4 ± 54.6^{a}	71.9 ± 19.5^{b}
PCNA/CD31	NE	177.9 ± 39.8	19.8 ± 5.4^{b}
Cdk2	18.0 ± 5.7	176 ± 40^{a}	73.5 ± 11.7^{b}

Data are mean $\pm$ SD. NE; not examined. The numbers of PCNA-positive cells, PCNA/CD31 double-positive cells, and Cdk2-expressing cells were determined in 10 fields of the submesothelial region selected at random at $\times400$ magnification.

[a] $P < 0.01$ vs. control group.
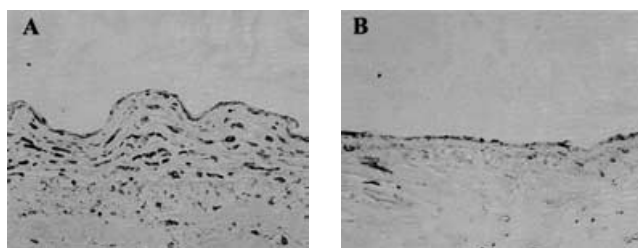
[b] $P < 0.01$ vs. CG group.

Fig. 7. Immunohistochemistry for Cdk2. Note the large number of Cdk2-positive cells in the CG group (*A*), but fewer such cells in CG+TNP470 group (*B*). Magnification: $\times200$.

cells, and expression pattern of Cdk2 was similar to that of PCNA in CG group. Compared with CG group, TNP-470 treatment reduced the number of Cdk2-expressing cells in the thickened submesothelial area (Fig. 7B). These data are summarized in Table 2.

DISCUSSION

In the present study, we demonstrated that administration of TNP-470 markedly reduced the number of blood vessels and myofibroblasts in the experimental mouse model induced by CG for peritoneal fibrosis. Moreover, treatment with TNP-470 diminished collagen accumulation in the thickened submesothelial area. These findings indicate that TNP-470 might be useful in preventing the progression of peritoneal fibrosis, and that angiogenesis is involved, at least in part, in the development of peritoneal fibrosis.

In this study, we demonstrated that administration of TNP-470 in CG-treated mice reduced the number of CD31-positive vessels in the thickened submesothelial area. TNP-470 exerts its antiangiogenic effect through the inhibition of endothelial cell proliferation and migration [16, 33, 34]. In fact, immunohistochemical staining for PCNA revealed that most of the vascular endothelial cells were proliferating in CG-injected mice, whereas the number of PCNA-positive vascular endothelial cells in thickened submesothelial area was comparatively lower in TNP-470–treated mice, accompanied by reduction of peritoneal fibrosis. Furthermore, we showed that Cdk-2,

a molecule associated with cell cycle, was also involved in the inhibitory action of TNP-470 on peritoneal fibrosis. Increased expression of Cdk2 in the thickened peritoneal tissue was suppressed by TNP-470. These findings suggest that the angioinhibitory action of TNP-470 is likely to be involved in the suppression of peritoneal fibrosis in our experimental model, although the relationship between angiogenesis and fibrosis remains an important issue.

In recent studies, accumulating evidences link inflammation to angiogenesis in a variety of chronic inflammatory diseases [14, 15], and the benefits of antiangiogenic agents have been demonstrated [35]. For instance, in both adjuvant arthritis and collagen-induced arthritis in rats, Brahn et al [19, 36] reported that TNP-470 prevented the development of arthritis and reversed the established disease. Taxol, which can induce endothelial cell apoptosis, was also effective in an animal model of arthritis [19, 37]. In chronic inflammation, antiangiogenic therapy results in anti-inflammatory responses, and its effect is probably mediated through several mechanisms. Increasing the vasculature in any tissue expands the route of ingress for immune cells into inflammatory sites [38]. In addition, vascular endothelial cells themselves are known to summon inflammatory cells (monocytes and neutrophils) through increased expression of adhesion molecules, including vascular endothelial cell adhesion molecule-1 [39, 40], intercellular adhesion molecule-1[41], and E- and P-selectins [42]. Thus, decreasing the vasculature and endothelial cells in vessels may reduce cell infiltration and delete a potent source of proinflammatory cytokines and chemokines in inflammatory sites. In the present study, we demonstrated that treatment with TNP-470 resulted in a reduction of the number of infiltrating macrophages concurrent with inhibition of progression of peritoneal fibrosis, which were induced by CG injection. In CG-induced peritoneal fibrosis model, it is suggested that angiogenesis observed in the thickened submesothelial area contributes to the progression of peritoneal inflammation, which leads to peritoneal fibrosis. These results allow us to speculate that decreased inflammatory responses were a consequence of the antiangiogenic property of TNP-470 and may explain the abrogation of qualitative fibrotic response during the progression of peritoneal fibrosis.

Our results also showed that TNP-470 treatment reduced the number of PCNA-positive nonendothelial fibroblast-like cells, as well as PCNA-positive endothelial cells in the thickened submesothelial area. These results suggest that administration of TNP-470 might have an antiproliferative effect on myofibroblasts in the thickened peritoneal tissues. In a previous in vivo study, administration of TNP-470 in rats with anti-Thy-1.1 antibody-induced glomerulonephritis resulted in the suppression of mesangial cell proliferation and extracellular matrix expansion in glomeruli [29]. In addition, Yan et al [28]

also documented that treatment with TNP-470 could prevent the progression of hepatic fibrosis by inhibiting the proliferation of hepatic stellate cells in a rat model of carbon tetrachloride- and dimethylnitrosamine-induced hepatic fibrosis. Interestingly, our results also showed a reduction of collagen accumulation in the submesothelial area of TNP-470–treated mice. One possible explanation for the inhibition of collagen accumulation by TNP-470 in our model could be drawn from the negative mitogenic effects of TNP-470 on myofibroblasts, which are the major source of collagen production [43, 44]. Our results showed that the expression of HSP47, a collagen-specific molecular chaperone [45], was decreased in the submesothelial area of TNP-470–treated mice. Therefore, prevention of peritoneal fibrosis in our model by TNP-470 can be explained by two mechanisms: (*1*) inhibition of angiogenesis; and (*2*) suppression of myofibroblast proliferation in the submesothelial area. In a previous study, Margetts et al [32] demonstrated a reduction of peritoneal-associated vessels by gene transfer therapy of angiostatin, a potent inhibitor of endothelial cell proliferation in an experimental model of peritoneal fibrosis induced by chronic infusion of PD solution. They also observed a reduction of submesothelial thickening, although such effect was not statistically significant. We postulate that the antiangiogenic and antiproliferative effects of TNP-470 may have a mutually potentiating effect in suppressing the progression of peritoneal fibrosis in our model.

In the present study, we induced peritoneal fibrosis by intraperitoneal injection of CG. CG-induced peritoneal fibrosis does not mimic peritoneal sclerosis or encapsulating peritoneal sclerosis observed in patients on long-term PD. The underlying mechanisms of encapsulating peritoneal sclerosis are not fully understood, making it a difficult disease to model. In the CG-induced peritoneal fibrosis model, the number of vessels was increased in the submesothelial area, together with collagen deposition and thickening of the peritoneum [30]. In addition, treatment with antisense oligonucleotide for HSP47 inhibited the thickening of submesothelial area, suppressed collagen deposition, and reduced the number of vessels in this model [31]. The results of these previous studies suggest a link between angiogenesis and the development of peritoneal fibrosis and collagen accumulation. Based on these properties, we used this model to investigate the efficacy of TNP-470 on peritoneal fibrosis. While we do not think that the CG-induced peritoneal fibrosis equates with human peritoneal fibrosis, our model does exhibit the key pathologic features of human peritoneal sclerosis, including increased expression of collagen type III, HSP47, and α-SMA, macrophage infiltration, and increased expression of VEGF. Thus, the pathologic mechanisms discerned in the mouse are worthy of consideration in human.

CONCLUSION

We demonstrated that TNP-470 has antiangiogenic and antiproliferative effects in a mouse model of chemically induced peritoneal fibrosis. Our results suggest that angiogenesis, together with fibroblast proliferation, is an important process in the pathologic progression of peritoneal fibrosis.

ACKNOWLEDGMENTS

Reprint requests to Yoko Yoshio, M.D., Division of Nephrology, Second Department of Internal Medicine, Nagasaki University School of Medicine, 1–7-1 Sakamoto, Nagasaki 852–8501, Japan.
E-mail: yyoshiwo@hotmail.com

REFERENCES

1. GANDHI VC, HUMAYUN HM, ING TS, *et al*: Sclerotic thickening of the peritoneal membrane in maintenance peritoneal dialysis patients. *Arch Intern Med* 140:1201–1203, 1980
2. HAUGLUSTAINE D, VAN MEERBEEK J, MONBALLYU J, *et al*: Sclerosing peritonitis with mural bowel fibrosis in a patient on long-term CAPD. *Clin Nephrol* 22:158–162, 1984
3. NAKAMOTO M: Pathogenesis of peritoneal fibrosis and peritoneal small vessel changes. *Perit Dial Int* 16(Suppl 1):S39–41, 1996
4. COLES GA, TOPLEY N: Long-term peritoneal membrane changes. *Adv Ren Replace Ther* 7:289–301, 2000
5. WILLIAMS JD, CRAIG KJ, TOPLEY N, *et al*: Morphologic changes in the peritoneal membrane of patients with renal disease. *J Am Soc Nephrol* 13:470–479, 2002
6. HONDA K, NITTA K, HORITA S, *et al*: Morphological changes in the peritoneal vasculature of patients on CAPD with ultrafiltration failure. *Nephron* 72:171–176, 1996
7. COMBET S, MIYATA T, MOULIN P, *et al*: Vascular proliferation and enhanced expression of endothelial nitric oxide synthase in human peritoneum exposed to long-term peritoneal dialysis. *J Am Soc Nephrol* 11:717–728, 2000
8. MATEIJSEN MA, VAN DER WAL AC, HENDRIKS PM, *et al*: Vascular and interstitial changes in the peritoneum of CAPD patients with peritoneal sclerosis. *Perit Dial Int* 19:517–525, 1999
9. ZWEERS MM, STRUIJK DG, SMIT W, *et al*: Vascular endothelial growth factor in peritoneal dialysis: A longitudinal follow-up. *J Lab Clin Med* 137:125–132, 2001
10. ZWEERS MM, DE WAART DR, SMIT W, *et al*: Growth factors VEGF and TGF-beta1 in peritoneal dialysis. *J Lab Clin Med* 134:124–132, 1999
11. FOLKMAN J: Tumor angiogenesis. *Adv Cancer Res* 43:175–203, 1985
12. D'AMORE PA: Growth factors, angiogenesis and metastasis. *Prog Clin Biol Res* 212:269–285, 1986
13. SEBAG J, MCMEEL JW: Diabetic retinopathy. Pathogenesis and the role of retina-derived growth factor in angiogenesis. *Surv Ophthalmol* 30:377–384, 1986
14. SCHRAA AJ, EVERTS M, KOK RJ, *et al*: Development of vasculature targeting strategies for the treatment of cancer and chronic inflammatory diseases. *Biotechnol Annu Rev* 8:133–165, 2002
15. STRIETER RM, BELPERIO JA, KEANE MP: CXC chemokines in angiogenesis related to pulmonary fibrosis. *Chest* 122:298S–301S, 2002
16. INGBER D, FUJITA T, KISHIMOTO S, *et al*: Synthetic analogues of fumagillin that inhibit angiogenesis and suppress tumour growth. *Nature* 348:555–557, 1990
17. LIEKENS S, VERBEKEN E, VANDEPUTTE M, *et al*: A novel animal model for hemangiomas: Inhibition of hemangioma development

by the angiogenesis inhibitor TNP-470. *Cancer Res* 59:2376–2383, 1999

18. JOUSSEN AM, BEECKEN WD, MOROMIZATO Y, *et al*: Inhibition of inflammatory corneal angiogenesis by TNP-470. *Invest Ophthalmol Vis Sci* 42:2510–2516, 2001

19. OLIVER SJ, BANQUERIGO ML, BRAHN E: Suppression of collagen-induced arthritis using an angiogenesis inhibitor, AGM-1470, and a microtubule stabilizer, taxol. *Cell Immunol* 157:291–299, 1994

20. OLIVER SJ, CHENG TP, BANQUERIGO ML, *et al*: Suppression of collagen-induced arthritis by an angiogenesis inhibitor, AGM-1470, in combination with cyclosporin: Reduction of vascular endothelial growth factor (VEGF). *Cell Immunol* 166:196–206, 1995

21. INOUE K, CHIKAZAWA M, FUKATA S, *et al*: Docetaxel enhances the therapeutic effect of the angiogenesis inhibitor TNP-470 (AGM-1470) in metastatic human transitional cell carcinoma. *Clin Cancer Res* 9:886–899, 2003

22. MIKI T, NONOMURA N, NOZAWA M, *et al*: Angiogenesis inhibitor TNP-470 inhibits growth and metastasis of a hormone-independent rat prostatic carcinoma cell line. *J Urol* 160:210–213, 1998

23. MORI S, UEDA T, KURATSU S, *et al*: Suppression of pulmonary metastasis by angiogenesis inhibitor TNP-470 in murine osteosarcoma. *Int J Cancer* 61:148–152, 1995

24. SINGH Y, SHIKATA N, KIYOZUKA Y, *et al*: Inhibition of tumor growth and metastasis by angiogenesis inhibitor TNP-470 on breast cancer cell lines in vitro and in vivo. *Breast Cancer Res Treat* 45:15–27, 1997

25. HORI A, IKEYAMA S, SUDO K: Suppression of cyclin D1 mRNA expression by the angiogenesis inhibitor TNP-470 (AGM-1470) in vascular endothelial cells. *Biochem Biophys Res Commun* 204:1067–1073, 1994

26. KRIA L, OHIRA A, AMEMIYA T: TNP-470 (a fungus-derived inhibitor of angiogenesis) reduces proliferation of cultured fibroblasts isolated from primary pterygia: A possible drug therapy for pterygia. *Curr Eye Res* 17:986–993, 1998

27. OGATA T, KURABAYASHI M, MAENO T, *et al*: Angiogenesis inhibitor TNP-470 (AGM-1470) suppresses vascular smooth muscle cell proliferation after balloon injury in rats. *J Surg Res* 112:117–121, 2003

28. WANG YQ, IKEDA K, IKEBE T, *et al*: Inhibition of hepatic stellate cell proliferation and activation by the semisynthetic analogue of fumagillin TNP-470 in rats. *Hepatology* 32:980–989, 2000

29. HARAGUCHI M, OKAMURA M, KONISHI M, *et al*: Anti-angiogenic compound (TNP-470) inhibits mesangial cell proliferation in vitro and in vivo. *Kidney Int* 51:1838–1846, 1997

30. MISHIMA Y, MIYAZAKI M, ABE K, *et al*: Enhanced expression of heat shock protein 47 in rat model of peritoneal fibrosis. *Perit Dial Int* 23:14–22, 2003

31. NISHINO T, MIYAZAKI M, ABE K, *et al*: Antisense oligonucleotides against collagen-binding stress protein HSP47 suppress peritoneal fibrosis in rats. *Kidney Int* 64:887–896, 2003

32. MARGETTS PJ, GYORFFY S, KOLB M, *et al*: Antiangiogenic and antifibrotic gene therapy in a chronic infusion model of peritoneal dialysis in rats. *J Am Soc Nephrol* 13:721–728, 2002

33. FIGG WD, PLUDA JM, LUSH RM, *et al*: The pharmacokinetics of TNP-470, a new angiogenesis inhibitor. *Pharmacotherapy* 17:91–97, 1997

34. ZHANG Y, GRIFFITH EC, SAGE J, *et al*: Cell cycle inhibition by the anti-angiogenic agent TNP-470 is mediated by p53 and p21WAF1/CIP1. *Proc Natl Acad Sci USA* 97:6427–6432, 2000

35. GRIFFIOEN AW, MOLEMA G: Angiogenesis: Potentials for pharmacologic intervention in the treatment of cancer, cardiovascular diseases, and chronic inflammation. *Pharmacol Rev* 52:237–268, 2000

36. PEACOCK DJ, BANQUERIGO ML, BRAHN E: A novel angiogenesis inhibitor suppresses rat adjuvant arthritis. *Cell Immunol* 160:178–184, 1995

37. ARSENAULT AL, LHOTAK S, HUNTER WL, *et al*: Taxol involution of collagen-induced arthritis: Ultrastructural correlation with the inhibition of synovitis and neovascularization. *Clin Immunol Immunopathol* 86:280–289, 1998

38. SOLOWIEJ A, BISWAS P, GRAESSER D, *et al*: Lack of platelet endothelial cell adhesion molecule-1 attenuates foreign body inflammation because of decreased angiogenesis. *Am J Pathol* 162:953–962, 2003

39. FRIES JW, WILLIAMS AJ, ATKINS RC, *et al*: Expression of VCAM-1 and E-selectin in an in vivo model of endothelial activation. *Am J Pathol* 143:725–737, 1993

40. PELLETIER RP, OHYE RG, VANBUSKIRK A, *et al*: Importance of endothelial VCAM-1 for inflammatory leukocytic infiltration in vivo. *J Immunol* 149:2473–2481, 1992

41. IKEDA U, IKEDA M, SEINO Y, *et al*: Expression of intercellular adhesion molecule-1 on rat vascular smooth muscle cells by proinflammatory cytokines. *Atherosclerosis* 104:61–68, 1993

42. KULIDJIAN AA, ISSEKUTZ AC, ISSEKUTZ TB: Differential role of E-selectin and P-selectin in T lymphocyte migration to cutaneous inflammatory reactions induced by cytokines. *Int Immunol* 14:751–760, 2002

43. GABBIANI G: The myofibroblast in wound healing and fibrocontractive diseases. *J Pathol* 200:500–503, 2003

44. PHAN SH: The myofibroblast in pulmonary fibrosis. *Chest* 122:286S–289S, 2002

45. NAKAI A, SATOH M, HIRAYOSHI K, *et al*: Involvement of the stress protein HSP47 in procollagen processing in the endoplasmic reticulum. *J Cell Biol* 117:903–914, 1992